Approach to enhance quantum gravity effects by ultimate acceleration

Huaiyang Cui
Department of Physics, Beihang University, Beijing, 102206, China
Email: hycui@buaa.edu.cn

Abstract: In analogy to the ultimate speed c, assume that there is an ultimate acceleration β, nobody's acceleration can exceed this limit β. By fitting observational data, it is found that the solar system has an ultimate acceleration of β=2.961520e+10(m/s/s), no rocket's acceleration can exceed this limit β. Because this ultimate acceleration is a large number, any effect connecting to β will become easy to test, including quantum gravity test. The ultimate acceleration makes a strict restriction on planet-rotation, it establishes a quantum rule for gravity, it is reported in this paper that the Sun and first four planets (Mercury, Venus, Earth, Mars) are quantized very well in accordance with the limit β. In other words, the ultimate acceleration β can derive out a generalized matter wave which causes the planetary quantization. Using the generalized matter wave and its Planck-constant-like constant, the solar system, Jupiter's satellites, Saturn's satellites, Uranus' satellites, Neptune's satellites as five different many-body systems are investigated with the Bohr orbit model. The calculation results agree well with experimental observations for these planets and satellites. This paper also discusses the possibility of applying the generalized matter wave to the Moon's orbit, tropic cyclone and virus.

1. Introduction

Today, quantum gravity has developed many different approaches. Many directions have led to significant advances with various appealing ideas; these include perturbative quantum gravity, nonperturbative quantum gravity, loop and string theory, etc. [1]. C. Marletto el al. proposed an experiment to detect the entanglement generated between two masses via gravitational interaction [2]. T. Guerreiro discussed the quantum mechanical description of a gravitational wave interacting with a cavity electromagnetic field [3]. Some quantum gravity proposals are extremely hard to test in practice, as quantum gravitational effects are appreciable only at the Planck scale.

The present paper suggests an approach to enhance the quantum gravity effect for test. For example, considering the assumption that there is an ultimate acceleration β, nobody's acceleration can exceed this limit β, the following section 3 shows β=2.961520e+10(m/s^2) in the solar system. Because this ultimate acceleration is a large number, any effect connecting to β will become easy to test, including quantum gravity test. In order to clarify the concept of ultimate acceleration, we first have to invoke the relativistic equality principle.

2. How to connect the ultimate acceleration with quantum gravity

(1) Pythagorean theorem and the relativity

In the relativity, the speed of light c is an ultimate speed, nobody's speed can exceed this limit c. The relativistic velocity u of a particle satisfies

$$u_1^2+u_2^2+u_3^2+u_4^2=-c^2\ . \tag{1}$$

No matter what particles (electrons, molecules, neutrons, quarks), their 4-vector velocities all have the same magnitude: $|u|=ic$. All particles gain **equality** because of the same magnitude of their 4-velocity u.

In an inertial frame, consider a particle of mass m with speed v, according to the **Pythagorean theorem**, in time interval dt the particle moves

$$dx_1^2+dx_2^2+dx_3^2=v^2dt^2 \tag{2}$$

Subtracting the both sides of the above equation by c^2dt^2, we get

$$dx_1^2+dx_2^2+dx_3^2-c^2dt^2=v^2dt^2-c^2dt^2 \tag{3}$$

It can be rewritten as

$$\left(\frac{dx_1}{dt}\right)^2+\left(\frac{dx_2}{dt}\right)^2+\left(\frac{dx_3}{dt}\right)^2-c^2\left(\frac{dt}{dt}\right)^2=-c^2(1-\frac{v^2}{c^2}) \tag{4}$$

We define the fourth axis and the proper time interval as

$$x_4=ict;\quad d\tau=\sqrt{1-v^2/c^2}\,dt \tag{5}$$

Then, the coordinates ($x_1,x_2,x_3,x_4=ict$) construct up the relativistic space-time in which the 4-vector velocity are specified by

$$u_1=\frac{dx_1/dt}{\sqrt{1-v^2/c^2}}\quad u_2=\frac{dx_2/dt}{\sqrt{1-v^2/c^2}}$$
$$u_3=\frac{dx_3/dt}{\sqrt{1-v^2/c^2}}\quad u_4=\frac{dx_4/dt}{\sqrt{1-v^2/c^2}} \tag{6}$$

We have

$$u_1^2+u_2^2+u_3^2+u_4^2=-c^2 \tag{7}$$

It means that the magnitude of 4-vector velocity for every particle takes the same value: $|u|=ic$ (constant imaginary number), this is called as the **velocity equality principle**.

According to the **Pythagorean theorem**, the acceleration a of a particle is

$$a_1^2+a_2^2+a_3^2=a^2;\quad (a_4=0;\quad \because x_4=ict) \tag{8}$$

Assume that particles have an ultimate acceleration β as limit, no particle can exceed this acceleration limit β. Subtracting the both sides of the above equation by β^2, we have

$$a_1^2+a_2^2+a_3^2-\beta^2=a^2-\beta^2;\qquad a_4=0 \tag{9}$$

It can be rewritten as

$$[a_1^{\ 2}+a_2^{\ 2}+a_3^{\ 2}+0+(i\beta)^2]\frac{1}{1-a^2/\beta^2}=-\beta^2 \tag{10}$$

Now, the particle subjects to an acceleration whose five components are specified by

$$\begin{aligned}&\alpha_1=\frac{a_1}{\sqrt{1-a^2/\beta^2}};\quad \alpha_2=\frac{a_2}{\sqrt{1-a^2/\beta^2}};\\ &\alpha_3=\frac{a_3}{\sqrt{1-a^2/\beta^2}};\quad \alpha_4=0;\quad \alpha_5=\frac{i\beta}{\sqrt{1-a^2/\beta^2}};\end{aligned} \tag{11}$$

where α_5 is the newly defined acceleration in five dimensional space-time ($x_1,x_2,x_3,x_4=ict,x_5$). Thus, we have

$$\alpha_1^2+\alpha_2^2+\alpha_3^2+\alpha_4^2+\alpha_5^2=-\beta^2;\quad \alpha_4=0 \tag{12}$$

It means that the magnitude of the newly defined acceleration α for every particle takes the same value: $|\alpha|=i\beta$ (constant imaginary number), this is called as the **acceleration equality principle**.

(2) Visualization of matter wave

How to resolve the velocity u and acceleration α into x, y, and z components? In realistic world, a hand can rotate a ball moving around a circular path at constant speed v with constant centripetal acceleration a, as shown in Fig.1(a).

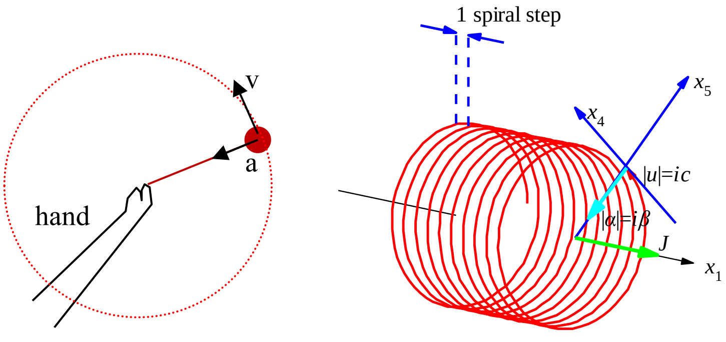

(a) (b) right hand chirality

Fig.1 (a) A hand rotates a ball moving around a circular path at constant speed v with constant centripetal acceleration a. (b) The particle moves along the x_1 axis with the constant speed $|u|=ic$ in the u direction and constant centripetal force in the x_5 axis at the radius iR (imaginary number).

```
<Clet2020 Script>//[26]
double D[100],S[2000];int i,j,R,X,N;
int main(){R=50;X=50;N=600;D[0]=-50;D[1]=0;D[2]=0;D[3]=X;D[4]=0;D[5]=0;D[6]=-50;D[7]=R;D[8]=0;
D[9]=600;D[10]=10;D[11]=R;D[12]=0;D[13]=3645;
Lattice(SPIRAL,D,S);SetViewAngle(0,80,-50);DrawFrame(FRAME_NULL,1,0xffffff);
Draw("LINE,0,2,XYZ,0","-150,0,0,-50,0,0");Draw("ARROW,0,2,XYZ,10","50,0,0,150,0,0");
SetPen(2,0xff0000);Plot("POLYLINE,0,600,XYZ",S[9]);i=9+3*N-6;Draw("ARROW,0,2,XYZ,10",S[i]);
TextHang(S[i],S[i+1],S[i+2],"   #if|u|=ic#t");TextHang(150,0,0,"   #ifx#sd1#t");SetPen(2,0x005fff);
Draw("LINE,1,2,XYZ,8","-50,0,50,-50,0,100");Draw("LINE,1,2,XYZ,8","-40,0,50,-40,0,100");
Draw("ARROW,0,2,XYZ,10","-80,0,100,-50,0,100");Draw("ARROW,0,2,XYZ,10","-10,0,100,-40,0,100");
TextHang(-50,0,110,"1 spiral step");i=9+3*N;S[i]=50;S[i+1]=10;S[i+2]=10;
Draw("ARROW,0,2,XYZ,10","50,0,0,50,80,80");TextHang(50,80,80," #ifx#sd5#t");
Draw("ARROW,0,2,XYZ,10","50,72,0,50,0,72");TextHang(50,0,72,"   #ifx#sd4#t");
SetPen(3,0x00ffff);Draw("ARROW,0,2,XYZ,15",S[i-3]);TextHang(S[i],S[i+1],S[i+2],"   #if|α|=iβ#t");
SetPen(3,0x00ff00);Draw("ARROW,0,2,XYZ,15","50,0,0,120,0,0");TextHang(110,5,5," #ifJ#t");
TextHang(-60,0,-80," right hand chirality");}#v07=?>A
```

In analogy with the ball in a circular path, consider a particle in one dimensional motion along the x_1 axis at the speed v, in the Fig.1(b) it moves with the constant speed $|u|=ic$ almost along the x_4 axis and slightly along the x_1 axis, and the constant centripetal acceleration $|\alpha|=i\beta$ in the x_5 axis at the constant radius iR (imaginary number); the coordinate system ($x_1, x_4=ict, x_5=iR$) establishes a cylinder coordinate system in which this particle moves spirally at the speed v along the x_1 axis. According to usual centripetal acceleration formula, the acceleration in the x_4-x_5 plane is given by

$$i\beta = \frac{|u|^2}{iR} = -\frac{c^2}{iR} = i\frac{c^2}{R} \quad . \tag{13}$$

Therefore, the track of the particle in the cylinder coordinate system ($x_1, x_4=ict, x_5=iR$) forms a shape, called as **acceleration-roll**. The faster the particle moves, the longer the spiral step is, while in the relativistic coordinate system ($x_1, x_4=ict$) the acceleration-roll is invisible due to lacking the x_5 axis.

As like a steel spring which contains elastic wave, the track in the acceleration-roll in Fig.1(b) can be described by a wave function whose phase changes 2π for one spiral step. The wave function phase changes 2π for one spiral circumferences $2\pi(iR)$, and the small displacement of the particle on the spiral track is $|u|d\tau = icd\tau$ in the 4-vector u direction, thus this wave phase along the spiral track is evaluated by

$$phase = \int_0^\tau \frac{2\pi}{2\pi(iR)} icd\tau = \int_0^\tau \frac{c}{R} d\tau \quad . \tag{14}$$

Substituting the radius R into it, the wave function ψ is given by

$$\psi = \exp(-i \cdot phase) = \exp(-i\int_0^\tau \frac{c}{R} d\tau) = \exp(-i\frac{\beta}{c}\int_0^\tau d\tau) \quad . \tag{15}$$

In the theory of relativity, we known that the integral along $d\tau$ needs to transform into realistic line integral, that is

$$\begin{aligned} d\tau &= -c^2 \frac{d\tau}{-c^2} = (u_1^2 + u_2^2 + u_3^2 + u_4^2)\frac{d\tau}{-c^2} \\ &= (u_1 dx_1 + u_2 dx_2 + u_3 dx_3 + u_4 dx_4)\frac{1}{-c^2} \end{aligned} \quad . \tag{16}$$

Therefore, the wave function ψ is evaluated by

$$\begin{aligned} \psi &= \exp(-i\frac{\beta}{c}\int_0^\tau d\tau) \\ &= \exp(i\frac{\beta}{c^3}\int_0^x (u_1 dx_1 + u_2 dx_2 + u_3 dx_3 + u_4 dx_4)) \end{aligned} \quad . \tag{17}$$

This wave function may have different explanations, depending on the particle under investigation. If the β is replaced by the Planck constant, the wave function of electrons is given by

$$\begin{aligned} &assume: \quad \beta = \frac{mc^3}{\hbar} \\ &\psi = \exp(\frac{i}{\hbar}\int_0^x (mu_1 dx_1 + mu_2 dx_2 + mu_3 dx_3 + mu_4 dx_4)) \end{aligned} \quad . \tag{18}$$

where $mu_4dx_4=-Edt$, it strongly suggests that the wave function is just the de Broglie's matter wave [4,5,6]. In Fig.1(b), the acceleration-roll of particle moves with two distinctions: right-hand chirality and left-hand chirality. The direction of the angular momentum J would be slightly different from the advance x_1 due to spiral precession. It is easy to calculate the ultimate acceleration β, the radius

R and the angular momentum J in the plane x_4-x_5 for spiraling electron as

$$\begin{aligned} \beta &= \frac{c^3 m}{\hbar} = 2.327421\text{e+29 (M/s}^2\text{)} \\ R &= \frac{c^2}{\beta} = 3.861593\text{e-13 (M)} \\ J &= \pm m\,|\,u\,|\,iR = \mp\hbar \end{aligned} \quad . \tag{19}$$

```
<Clet2020 Script>//[26]
double beta,R,J,m,D[10];char str[200];
int main(){m=ME;beta=SPEEDC*SPEEDC*SPEEDC*m/PLANCKBAR;
R=SPEEDC*SPEEDC/beta;J=PLANCKBAR;Format(str,"beta=%e, #nR=%e, #nJ=%e",beta,R,J);
TextAt(50,50,str);ClipJob(APPEND,str);}#v07=#t
```

The wave function ψ in Eq.(17) is a pure geometry wave. Considering planets in the solar system, no Planck constant can be involved. In a many-body system with the total mass M, the ultimate acceleration can be rewritten in terms of **Planck-constant-like constant** h as

$$\begin{aligned} & assume: \quad \beta = \frac{c^3}{hM} \\ & \psi = \exp\left(\frac{i}{hM}\int_0^x (u_1 dx_1 + u_2 dx_2 + u_3 dx_3 + u_4 dx_4)\right) \end{aligned} \quad . \tag{20}$$

The constant h will be determined by experimental observations. In next section we shall try to use this wave function as the planetary scale waves in the solar system to explain quantum gravity effects for the planets and satellites [7—25], the wave function is called as the **acceleration-roll wave**.

Tip: actually, ones cannot get to see the acceleration-roll of particle in the relativistic space-time ($x_1,x_2,x_3,x_4=ict$) ; only get to see it in the cylinder coordinate system ($x_1,x_4=ict,x_5=iR$).[28]

(3) Position equality principle

Position, velocity and acceleration are three basic concepts in particle physics, correspondingly, we have the position equality principle, the velocity equality principle, and the acceleration equality principle, respectively. The **position equality principle** admits there exists an **ultimate distance** D which is automatically recognized as the diameter of our universe: among the D rang nobody can escape. The position equality principle provides us a useful insight into cosmic microwave background, the Hubble law and dark matter.

Consider a star that have distance r to the sun (to us), we establish a frame of reference with the origin at the sun, as shown in Fig.2 in the Cartesian coordinates (x,y,z), the Pythagorean theorem tells us

$$x^2 + y^2 + z^2 = r^2 \tag{21}$$

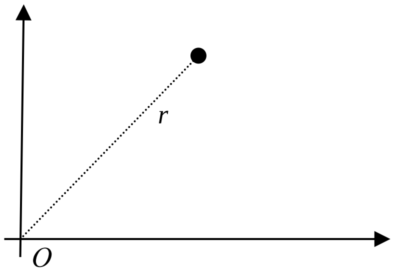

Fig.2 A star in the solar reference frame.

Because the distance is a very large quantity for the star, we worry about non-Euclidian effect that may involve within, we modify it as

$$x^2+y^2+z^2=r^2+kr \tag{22}$$

where the kr term represents the possible non-Euclidian effect. Suppose there is the ultimate distance D in the universe, then we have

$$\begin{aligned} x^2+y^2+z^2-D^2 &= -D^2+r^2+kr \\ x^2+y^2+z^2-D^2 &= -D^2\left(1-\frac{kr}{D^2}-\frac{r^2}{D^2}\right) \end{aligned} \tag{23}$$

It can be rewritten as

$$\begin{aligned} &\left(\frac{x}{\sqrt{1-kr/D^2-r^2/D^2}}\right)^2+\left(\frac{y}{\sqrt{1-kr/D^2-r^2/D^2}}\right)^2 \\ &+\left(\frac{z}{\sqrt{1-kr/D^2-r^2/D^2}}\right)^2+\left(\frac{iD}{\sqrt{1-kr/D^2-r^2/D^2}}\right)^2=-D^2 \end{aligned} \tag{24}$$

Then, new coordinates can be established, are specified by

$$\begin{aligned} x' &= \frac{x}{\sqrt{1-kr/D^2-r^2/D^2}} \quad & y' &= \frac{y}{\sqrt{1-kr/D^2-r^2/D^2}} \\ z' &= \frac{z}{\sqrt{1-kr/D^2-r^2/D^2}} \quad & d' &= \frac{iD}{\sqrt{1-kr/D^2-r^2/D^2}} \end{aligned} \tag{25}$$

In the new coordinates (x',y',z',d'), all stars to the origin are the same for their same distance:

$$|x'^2+y'^2+z'^2+d'^2|=iD \tag{26}$$

The magnitude of the distance is a constant! It is in analogy with the velocity equality principle in the relativistic space-time. The new coordinates (x',y',z',d') is named as the **position equality space** in the followings. The above equation is called as the **position equality principle**.

Notice that a star moving at the classical position (x,y,z) will never be able escape from us in the position equality space (x',y',z',d'), simply because

$$
\begin{aligned}
x' &= \frac{x}{\sqrt{1-kr/D^2-r^2/D^2}} \quad \Rightarrow \quad |x'|<D \\
y' &= \frac{y}{\sqrt{1-kr/D^2-r^2/D^2}} \quad \Rightarrow \quad |y'|<D \\
z' &= \frac{z}{\sqrt{1-kr/D^2-r^2/D^2}} \quad \Rightarrow \quad |z'|<D
\end{aligned} \tag{27}
$$

In other words, all distance stars are confined in an equivalent cavity with the diameter D. Our universe is a blackbody cavity in terms of the position equality principle, in which all electromagnetic radiations warm up our universe, as shown in Fig.3.

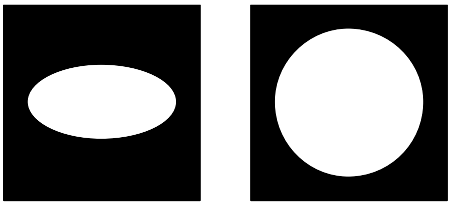

Fig.3 A classical cavity, and an equivalent cavity confined by $r<D$ in the position equality space (x',y',z',d').

```
<Clet2020 Script>//[26]
int i,j,k,nP[10];
double r,x,y,z,dP[10],D[10];
int main(){DrawFrame(FRAME_NULL,1,0xafffaf); r=40;x=-50;D[0]=x-r;D[1]=-r;D[2]=x+r;D[3]=r;
SetPen(1,0x000000); Draw("RECT,1,2,XY,10",D); x=50;r=40;D[0]=x-r;D[1]=-r;D[2]=x+r;D[3]=r;
Draw("RECT,1,2,XY,10",D); r=30;x=-50;D[0]=x-r;D[1]=-r/2;D[2]=x+r;D[3]=r/2;
Draw("ELLIPSE,3,2,XY,0xffffff",D); r=30;x=50;D[0]=x-r;D[1]=-r;D[2]=x+r;D[3]=r;
Draw("ELLIPSE,3,2,XY,0xffffff",D);
TextHang(-x-x,-x,0,"classical cavity");TextHang(0,-x,0,"cavity confined by r<D");
}#v07=?>A
```

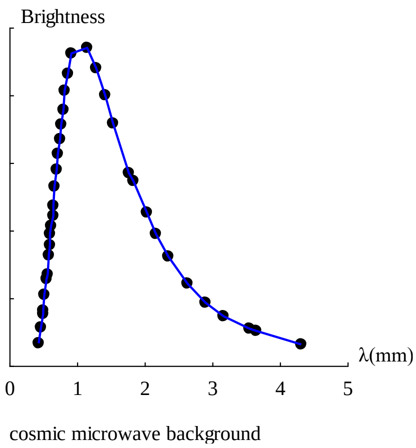

Fig.4 The measurement of the cosmic microwave background.

```
<Clet2020 Script>//[26]
int i,j,k,nP[10];char str[100]; double
D[74]={0.44,6.53,0.48,11.04,0.51,15.09,0.51,16.17,0.53,21.00,0.56,25.51,0.57,26.91,0.59,32.50,0.60,35.46,0.61,38.72,0.62,41.0
6,0.65,44.32,0.66,47.28,0.68,52.88,0.70,57.85,0.72,62.36,0.76,66.87,0.77,71.07,0.80,75.43,0.83,81.18,0.87,86.31,0.93,92.07,1.1
6,93.78,1.29,87.87,1.42,79.94,1.54,71.54,1.78,56.92,1.84,54.43,2.04,45.26,2.18,38.72,2.36,32.19,2.64,24.11,2.90,18.66,3.17,14.
62,3.56,10.73,3.65,10.11,4.33,6.22,};
int main(){ SetAxis(X_AXIS,0,0,5,"λ(mm);0;1;2;3;4;5;");SetAxis(Y_AXIS,0,0,100,"Brightness;;;;;;;");
DrawFrame(FRAME_SCALE,1,0xafffaf); Plot("OVALFILL,0,37,XY,5,5,",D);
SetPen(2,0x0000ff); Polyline(37,D); TextHang(0,-20,0,"cosmic microwave background");
}#v07=?>A
```

According to the blackbody theory, our universe has a mean temperature T with a standard blackbody spectrum in the cavity $r<D$, experimental observations confirmed the profile of cosmic microwave background radiation to be an exact blackbody radiation spectrum at the temperature T=2.725K, as shown in Fig.4.

Now, let us test the position equality principle using the Hubble law. Consider an atom at far distance $x=r$, emitting an electromagnetic wave of wavelength λ. We must hold the position equality principle for all stars, so actually we live in the new coordinate system (x',y',z',d'), what we see is

$$\begin{aligned} x' &= \frac{x}{\sqrt{1-kr/D^2-r^2/D^2}} \qquad dx' \simeq (1+\frac{kr}{2D^2})dx \\ y' &= y = 0 \\ z' &= z = 0 \\ d' &= \frac{iD}{\sqrt{1-kr/D^2-r^2/D^2}} \end{aligned} \tag{28}$$

Thus, we at the origin receive the wave length λ' of the electromagnetic wave as

$$\lambda' \simeq (1+\frac{kr}{2D^2})\lambda \tag{29}$$

This is the Hubble law for far stars, the $2D^2/k$ equals to the Hubble constant, in fact the Hubble law happens in all directions in the sky like cosmic microwave background in all directions. The advantage of the position equality principle is that it is not necessary for stars to recede as prediction by the Doppler effect theory for frequency shift. For last many decades, our vision to the cosmology has been misguided by abuse of the Doppler effect for electromagnetic wave over the Hubble law, the later leads to the expansion of the universe and the big bang. Now, sleeping with the position equality principle, it is time for the universe to become quiet [28].

3. The acceleration-roll wave in planetary systems

In the preceding section, we have defined the generalized matter wave as the acceleration-roll wave, which is a pure geometry wave based on the equality principle.

In a many-body system with the total mass M, a constituent particle has the mass m and moves at the speed v, its wavelength of matter wave is modified in Eq.(20) as

$$\lambda = \frac{2\pi\hbar}{mv} \Rightarrow \text{modify} \Rightarrow \lambda = \frac{2\pi hM}{v} \ . \tag{30}$$

where h is a Planck-constant-like constant. It is found that this modified matter wave works for quantizing orbits correctly [28,29].

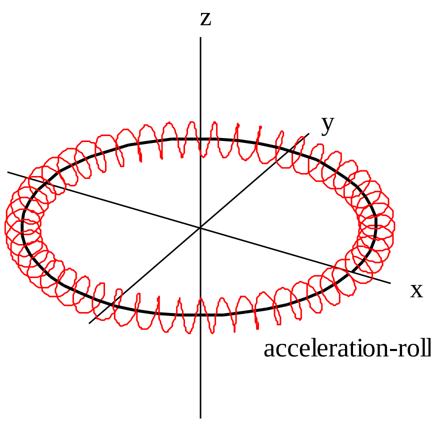

Fig.5 A planet 2D orbit around the sun, an acceleration-roll winding around the planet.

```
<Clet2020 Script>//[26]
int i,j,k; double r,rot,x,y,z,D[20],F[20],S[200];
int main(){SetViewAngle("temp0,theta60,phi-30");
DrawFrame(FRAME_LINE,1,0xafffaf);r=80;Spiral(); TextHang(r,-r,0,"acceleration-roll");
r=110;TextHang(r,0,0,"x");TextHang(0,r,0,"y");TextHang(0,0,r,"z");}
Spiral(){r=80;j=10;rot=j/r;k=2*PI/rot+1;
for(i=0;i<k;i+=1) {D[0]=x;D[1]=y;D[2]=z;D[6]=x;D[7]=y;D[8]=r;
x=r*cos(rot*i);y=r*sin(rot*i);z=0;if(i==0) continue;
SetPen(2,0x00);F[0]=D[0];F[1]=D[1];F[2]=x;F[3]=y;Draw("LINE,0,2,XY,",F);SetPen(1,0xff0000);
D[3]=x;D[4]=y;D[5]=z; D[9]=40;D[10]=10;D[11]=8;D[12]=0;D[13]=360;
Lattice(SPIRAL,D,S);Plot("POLYLINE,0,40,XYZ",S[9]);}
}#v07=?>A
```

In the Bohr's orbit model, as shown in Fig.5, the circular quantization condition is given by

$$\left.\begin{aligned} 2\pi r = n\lambda; \quad \lambda = 2\pi hM / v \\ v = \sqrt{\frac{GM}{r}} \end{aligned}\right\} \quad \Rightarrow \quad \sqrt{r} = h\sqrt{\frac{M}{G}}n \tag{31}$$

It indicates that there is a linear relation between the square root of radius and the quantum number n. The solar system, Jupiter's satellites, Saturn's satellites, Uranus' satellites, Neptune's satellites as five different many-body systems are investigated with the Bohr's orbit model. After fitting observational data, the Planck-constant-like constant h is obtained in Table 1, respectively, the predicted quantization in Fig.6(a), Fig.6(b), Fig.6(c), Fig.6(d) and Fig.6(e) agrees well with experimental observations for those inner constituent particles. The key point is that the various systems have almost same Planck-constant-like constant h in Table 1 with a mean value of 3.51e-16 $m^2s^{-1}kg^{-1}$, at least have the same magnitude!

Table 1 Planck-constant-like constant h in various systems, N is constituent particle number with smaller inclination.

system	N	h ($m^2s^{-1}kg^{-1}$)	M/M_{earth}	Prediction
Solar planets	9	4.574635e-16	333000	Fig.6(a)
Jupiter' satellites	7	3.531903e-16	318	Fig.6(b)
Saturn's satellites	7	6.610920e-16	95	Fig.6(c)
Uranus' satellites	18	1.567124e-16	14.5	Fig.6(d)
Neptune 's satellites	7	1.277170e-16	17	Fig.6(e)

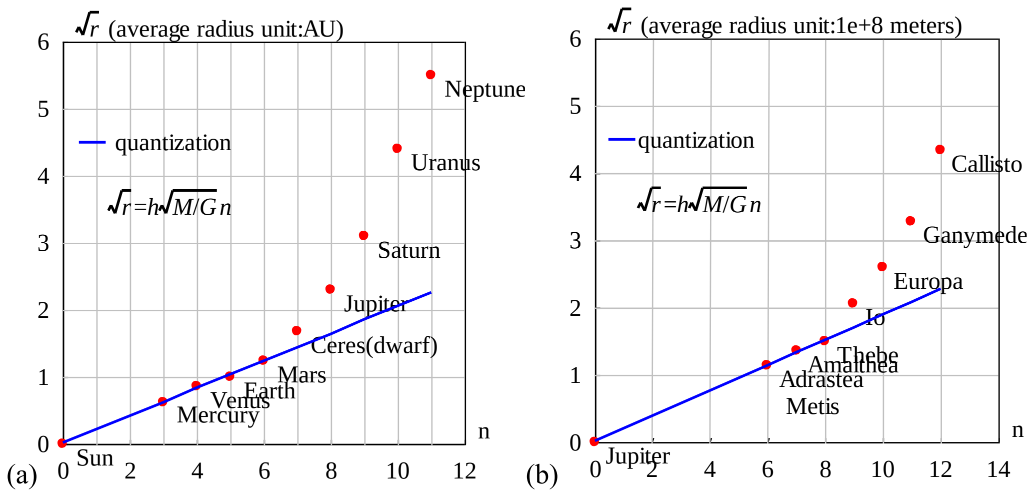

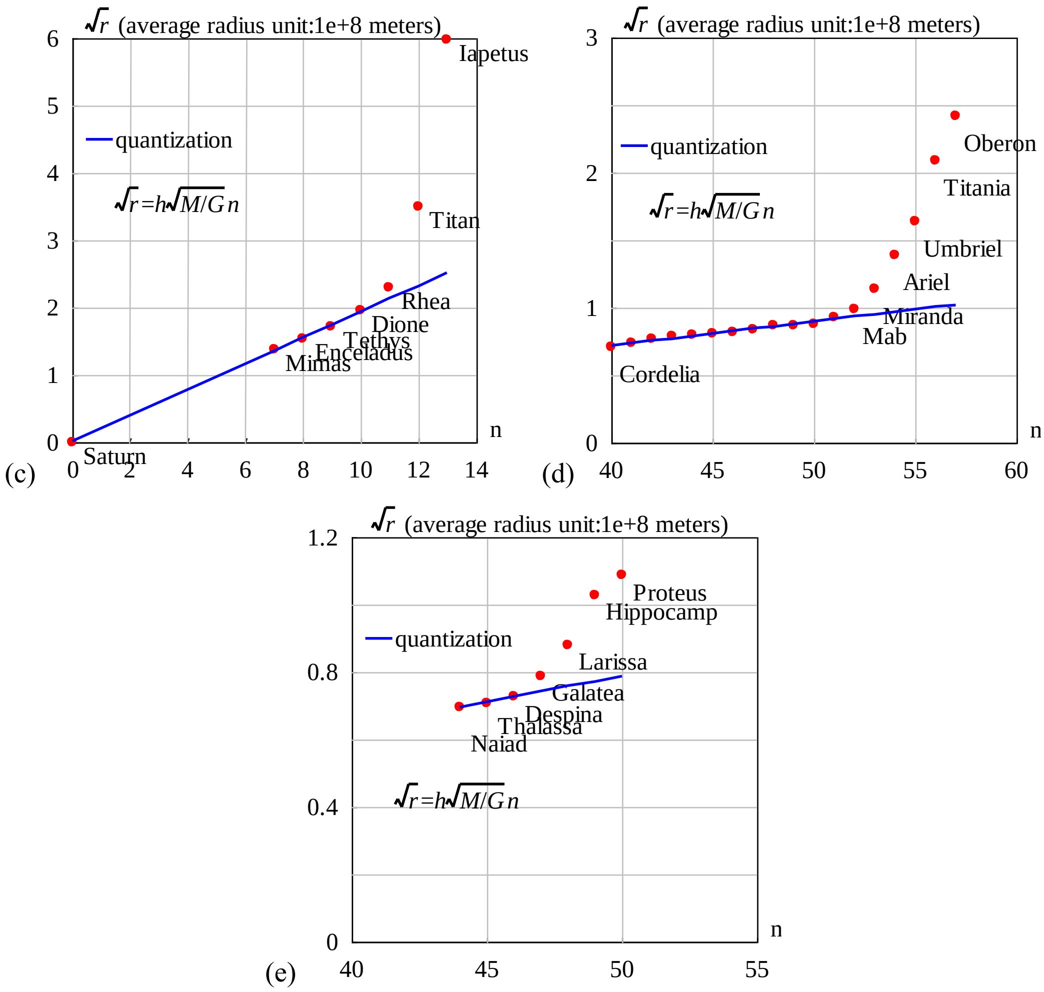

Fig.6 The orbital radii are quantized for inner constituents. (a) the solar system with h=4.574635e-16 (m^{2}s^{-1}kg^{-1}). The relative error is less than 3.9%. (b) the Jupiter system with h=3.531903e-16 (m^{2}s^{-1}kg^{-1}). Metis and Adrastea are assigned the same quantum number for their almost same radius. The relative error is less than 1.9%.(c) the Saturn system with h=6.610920e-16 (m^{2}s^{-1}kg^{-1}). The relative error is less than 1.1%.(d) the Uranus system with h=1.567124e-16 (m^{2}s^{-1}kg^{-1}). n=0 is assigned to the Uranus. The relative error is less than 2.5%.(e) the Neptune system with h=1.277170e-16 (m^{2}s^{-1}kg^{-1}). n=0 is assigned to the Neptune. The relative error is less than 0.17%.

In Fig.6(a), the blue straight line expresses the linear regression relation among the Sun, Mercury, Venus, Earth and Mars, their quantization parameters are hM=9.098031e+14(m^2/s). The ultimate acceleration is β=2.961520e+10 (m/s^2). The quantization linear regression relation is independent from individual planetary mass and size.

4. Discussion: Moon, tropic cyclone and virus

The Moon is Earth's only proper natural satellite. It is one-quarter the diameter of Earth, making it the largest natural satellite in the solar system relative to the size of its planet. Earth had five known quasi-satellites.

Applying the linear regression relation of orbit quantization to the Moon, we obtain Fig.7(a). According to fitting-calculation, the ultimate acceleration is β=1.377075e+14 (m/s^2), the corresponding Planck-constant-like constant is h=3.276105e-14 (m^2/skg), indicating that h in this case may rise as the total mass M drops comparing to other planets. Another consideration is to take the quasi-satellite's perigee into account, for the moon and 2004_GU9 etc., as shown in Fig.7(b). But this consideration requires further understanding to quasi-satellites [28].

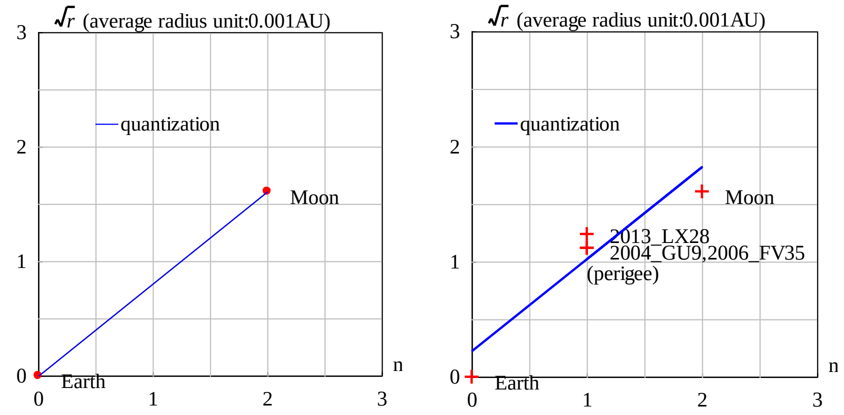

(a) H=1.956611e+11 B=0.000000e+00 (b) H=1.956611e+11 B=-5.221444e+10

Fig.7 orbital quantization for moon to the Earth.

```
<Clet2020 Script>//[26]
char str[200];int i,j,k,N,nP[10]; double x,y,z,M,r_unit,a,b,B,H,r_ave[20],dP[10],D[1000];
double orbit[10]={0,2.57,0,}; double e[10]={0, 0.0549,0,0,0,0,0,0,0,0,};
int qn[10]={0,2,3,4,5,6,7,8,9.,10,};
char Stars[100]={"Earth;Moon;"};
int main(){ N=2; M=5.97237E24; r_unit=1.495978707e8;
for(i=0;i<N;i+=1) {x=orbit[i];y=e[i]; z=x*(1+sqrt(1-y*y))/2;r_ave[i]=z;//average_radius
D[i+i]=qn[i];D[i+i+1]=sqrt(z); }
DataJob("REGRESSION,2",D,dP);b=dP[0];a=dP[1];
SetAxis(X_AXIS,0,0,3,"n;0;1;2;3;");
SetAxis(Y_AXIS,0,0,3," #if#rsr#t (average radius unit:0.001AU);0;1;2;3;");
DrawFrame(0x0166,1,0xafffaf); Polyline(N,D);
SetPen(2,0xff0000); Plot("OVALFILL,0,2,XY,3,3,",D);
for(i=0;i<N;i+=1) {nP[0]=TAKE;nP[1]=i;TextJob(nP,Stars,str);x=qn[i]+0.2;y=sqrt(orbit[i])-0.05;TextHang(x,y,0,str);}
x=GRAVITYC*M*r_unit;z=sqrt(x);H=z*a;B=-z*b;
TextAt(100,450,"#ifH#t=%e   #ifB#t=%e",H,B);
for(i=0;i<N;i+=1) {y=b+a*qn[i];D[i+i]=qn[i];D[i+i+1]=y;}
SetPen(1,0x0000ff);Polyline(N,D,0.5,2.2,"quantization");//check
}}#v07=?>A
```

In contrast with the stiff Planck constant for electrons, planetary Planck-constant-like constant can dramatically vary to a certain value to adapt to its dense constituents in a many-body system, so that this acceleration-roll wave with an adaptive wavelength can be applied to a variety of collective particles such as water-vapor, cloud, atmosphere, asteroids, space debris, etc. as shown in Fig.8. For example, we would make an attempt to use the acceleration-roll wave to describe tornados whose wavelength drops to about 1 meters or tropic cyclones whose wavelength drops to about 10---100 kilometers [28].

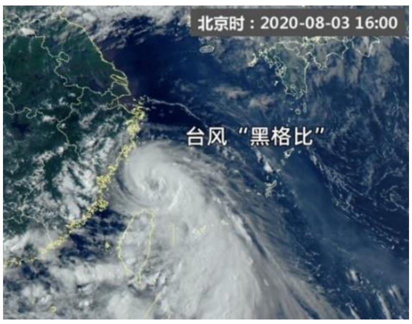

Fig.8 A typhoon in China, August 2020. [FY-4A satellite picture].

In recent years, virus COVID-19 has become a hot issue that is deserved to discuss.

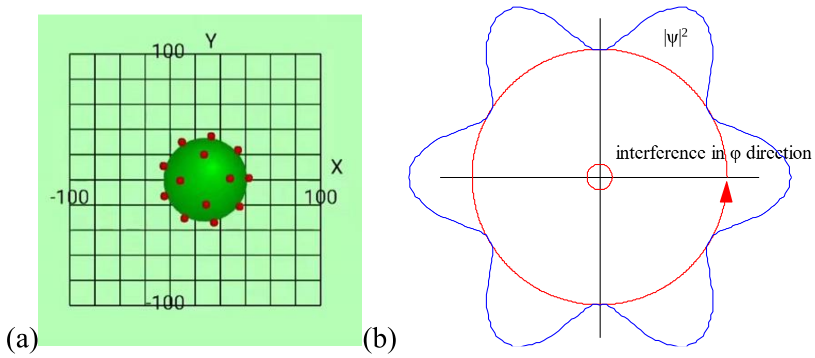

Fig.9 The molecular vibration in the r direction will grow out many spike glycoproteins on the surface of a virus. (b)the k_φ should be in constructed interference.

```
<Clet2020 Script>//[26]
int i,j,k,r;double a,b,D[1000];int nP[10];
int main(){DrawFrame(FRAME_LINE,1,0xafffaf);r=8;D[0]=-r;D[1]=-r;D[2]=r;D[3]=r;
nP[0]=OVAL;nP[1]=0x3003;nP[2]=2;nP[3]=XY;nP[4]=20;
SetPen(1,0xff0000);Draw(nP,D);nP[0]=SECTOR;nP[1]=3;nP[2]=3;nP[3]=XY;nP[4]=20;nP[5]=0;nP[6]=358;
D[0]=0;D[1]=0;D[2]=80;D[3]=0;D[4]=80;D[5]=0;Draw(nP,D);SetPen(1,0x0000ff);
TextHang(10,15,0,"interference in φ direction");TextHang(40,90,0,"|ψ|#su2#t");
k=360;a=2*PI/k;b=12*PI/k;j=0;for(i=0;i<=k;i+=1) {r=100+20*cos(b*i);
D[j+j]=r*cos(i*a);D[j+j+1]=r*sin(i*a);j+=1;}nP[0]=POLYLINE;nP[1]=0;nP[2]=k+1;nP[3]=XY;
nP[4]=0;nP[5]=0;nP[6]=0;Plot(nP,D);}#v07=?>A
```

As we know, the wavelength of a generalized matter wave (acceleration-roll wave) is given by

$$\lambda = \frac{2\pi\hbar}{mv} \quad \Rightarrow \text{modify} \Rightarrow \quad \lambda = \frac{2\pi hM}{v} \,. \tag{32}$$

Since the Earth's h= 3.276105e-14(m^2/skg), if a COVID-19 virus has a mass of 1e-9kg, then the virus' constant is estimated as hM = 3.276105e-23(m^2/s). To this estimation, the planetary scale h seems to be not suitable for the virus; but, actually, the virus' constant hM must adapt to itself and its environment. Suppose a virus has a radius of r, its acceleration-roll wave has wave vectors k_φ and k_r in a polar coordinate system (r,φ) fixed at the virus. As a 2D model, inside the virus body, its acceleration-roll in the φ direction must be in destructed interference, that is

$$\oint_L k_\varphi (r d\varphi) < \pi \,. \tag{33}$$

On the virus surface, k_φ should be in constructed interference in a form of standing wave, that is

$$\oint_L k_\varphi (r d\varphi) = \pi n \quad \Rightarrow \quad k_\varphi = \frac{n}{2r} \,. \tag{34}$$

The constructed interference is illustrated in Fig.9(b), where the quantum number n is also the node number n=5 for the standing wave on the surface. Suppose the virus surface has a rotating speed v, then the virus' Planck-constant-like constant is estimated as

$$k_\varphi = \frac{2\pi}{\lambda} = \frac{v}{hM} = \frac{n}{2r} \quad \Rightarrow \quad h = \frac{2rvM}{n} = \frac{2J}{n} \,. \tag{35}$$

where J=rvM represents approximately the angular momentum of the virus; if J is a small quantity, it is hard to find virus wave behavior. To note that there are several spikes of $|\psi|^2$ around the core in Fig.9(b), which manifests that virus is easy to grow out protein-spikes under the constructed interference of its acceleration-roll wave in the φ direction [28].

The acceleration-roll wave is a pure geometry wave, which can be applied to any geometry structures such as viruses, cells, animals, etc.

5. Conclusions

In analogy to the ultimate speed c, assume that there is an ultimate acceleration β, nobody's acceleration can exceed this limit β. By fitting observational data, it is found that the solar system has an ultimate acceleration of β=2.961520e+10(m/s/s), no rocket's acceleration can exceed this limit β. Because this ultimate acceleration is a large number, any effect connecting to β will become easy to test, including quantum gravity test. The ultimate acceleration makes a strict restriction on planet-rotation, it establishes a quantum rule for gravity, it is reported in this paper that the Sun and first four planets (Mercury, Venus, Earth, Mars) are quantized very well in accordance with the limit β. In other words, the ultimate acceleration β can derive out a generalized matter wave which causes the planetary quantization. Using the generalized matter wave and its Planck-constant-like constant, the solar system, Jupiter's satellites, Saturn's satellites, Uranus' satellites, Neptune's satellites as five different many-body systems are investigated with the Bohr orbit model. The calculation results agree well with experimental observations for these planets and satellites. This paper also discusses the possibility of applying the generalized matter wave to the Moon's orbit, tropic cyclone and virus.

References

[1]S. Carlip, D. Chiou, W. Ni, R. Woodard, Quantum Gravity: A Brief History of Ideas and Some Prospects, International Journal of Modern Physics D, V,24,14,2015,1530028. DOI:10.1142/S0218271815300281.

[2]C. Marletto, and V. Vedral, Gravitationally Induced Entanglement between Two Massive Particles is Sufficient Evidence of Quantum Effects in Gravity, Phys. Rev. Lett., 119, 240402 (2017)

[3]T. Guerreiro, Quantum effects in gravity waves, Classical and Quantum Gravity, 37 (2020) 155001 (13pp).

[4]de Broglie, L., CRAS,175(1922):811-813, translated in 2012 by H. C. Shen in Selected works of de Broglie.

[5]de Broglie, Waves and quanta, Nature, 112, 2815(1923): 540.

[6]de Broglie, Recherches sur la théorie des Quanta, translated in 2004 by A. F. Kracklauer as De Broglie, Louis, On the Theory of Quanta. 1925.

[7]NASA, https://solarscience.msfc.nasa.gov/interior.shtml.

[8]NASA, https://nssdc.gsfc.nasa.gov/planetary/factsheet/marsfact.html.

[9]B. Ryden Introduction to Cosmology, Cambridge University Press, 2019, 2nd edition.

[10]D. Valencia, D. D. Sasselov,R. J. O'Connell, Radius and structure models of the first super-earth planet, The Astrophysical Journal, 656:545-551, 2007, February 10.

[11]D. Valencia, D. D. Sasselov,R. J. O'Connell, Detailed models of super-earths: how well can we infer bulk properties? The Astrophysical Journal, 665:1413–1420, 2007 August 20.

[12]T. Guillot, A. P. Showman, Evolution of "51Pegasusb-like" planets, Astronomy & Astrophysics,2002, 385,156-165, DOI: 10.1051/0004-6361:20011624

[13]T. Guillot, A. P. Showman, Atmospheric circulation and tides of "51Pegasusb-like" planets, Astronomy & Astrophysics,2002, 385,166-180, DOI: 10.1051/0004-6361:20020101

[14]L.N. Fletcher,Y.Kaspi,T. Guillot, A.P. Showman, How Well Do We Understand the Belt/Zone Circulation of Giant Planet Atmospheres? Space Sci Rev, 2020,216:30. https://doi.org/10.1007/s11214-019-0631-9

[15]Y. Kaspi, E. Galanti, A.P. Showman, D. J. Stevenson, T. Guillot, L. Iess, S.J. Bolton, Comparison of the Deep Atmospheric Dynamics of Jupiter and Saturn in Light of the Juno and Cassini Gravity Measurements,Space Sci Rev, 2020, 216:84. https://doi.org/10.1007/s11214-020-00705-7

[16]Orbital Debris Program Office, HISTORY OF ON-ORBIT SATELLITE FRAGMENTATIONS, National Aeronautics and Space Administration, 2018, 15 th Edition.

[17]M. Mulrooney, The NASA Liquid Mirror Telescope, Orbital Debris Quarterly News, 2007, April,v11i2,
[18]Orbital Debris Program Office, Chinese Anti-satellite Test Creates Most Severe Orbital Debris Cloud in History, Orbital Debris Quarterly News, 2007, April,v11i2,
[[19]A. MANIS, M. MATNEY, A.VAVRIN, D. GATES, J. SEAGO, P. ANZ-MEADOR, Comparison of the NASA ORDEM 3.1 and ESA MASTER-8 Models, Orbital Debris Quarterly News, 2021, Sept,v25i3.
[20]D. Wright, Space debris, Physics today,2007,10,35-40.
[21]TANG Zhi-mei, DING Zong-hua, DAI Lian-dong, WU Jian, XU Zheng-wen, "The Statistics Analysis of Space Debris in Beam Parking Model in 78° North Latitude Regions," Space Debris Research, 2017, 17,3, 1-7.
[22]TANG Zhimei DlNG, Zonghua, YANG Song, DAI Liandong, XU Zhengwen, WU Jian The statistics analysis 0f space debris in beam parking model based On the Arctic 500 MHz incoherent scattering radar, CHINESE JOURNAL 0F RADIO SCIENCE, 2018, 25,5, 537-542
[23]TANG Zhimei， DING, Zonghua， DAI Liandong， WU Jian， XU Zhengwen, Comparative analysis of space debris gaze detection based on the two incoherent scattering radars located at 69N and 78N, Chin．J．Space Sci, 2018 38,1, 73-78. DOI:10.11728/cjss2018.01.073
[24]DING Zong-hua, YANG Song, JIANG hai, DAI Lian-dong, TANG Zhi-mei, XU Zheng-wen, WU Jian, The Data Analysis of the Space Debris Observation by the Qujing Incoherent Scatter Radar, Space Debris Research, 2018, 18,1, 12-19.
[19]Yang Chenwei, Jiang Peng, Jia Minghao, Zhou Xu, Zhang Shaohua, Zhou Hongyan, Li Gongqiang , Jiang Hai, Cheng Haowen , Liu Jing, Li Zhengyang, Station characteristics and CSTAR data measurement of LEO space-debris monitoring at Kunlun station, Antarctica, Chinese Journal of Polar research, 2019 31,2, 128-133.
[25]YANG Song, DING Zonghua, Xu Zhengwe, WU Jian, Statistical analysis on the space posture, distribution, and scattering characteristic of debris by incoherent scattering radar in Qujing, Chinese Journal of Radio science, 2018 33,6 648-654, DOI:10.13443/j.cjors.2017112301
[26]Clet Lab, Clet: a C compiler, https://drive.google.com/file/d/1OjKqANcgZ-9V5 6rgcoMtOu9w4rP49sgN/view?usp=sharing
[27] Huaiyang Cui, Relativistic Matter Wave and Its Explanation to Superconductivity: Based on the Equality Principle, Modern Physics, 10,3(2020)35-52. https://doi.org/10.12677/MP.2020.103005
[28]Huaiyang Cui, Relativistic Matter Wave and Quantum Computer, Kindle ebook, 2021.
[29]Huaiyang Cui, Evidence of Planck-Constant-Like Constant in Five Planetary Systems and Its Significances, viXra:2204.0133, 2022.